Analysis for Sectoral Microstrip Antennas for Varying Angle

Amit A. Deshmukh
Professor and Head, EXTC
DJSCOE
Vile Parle, Mumbai, India

Neelam V. Phatak, S.B. Nagarbowdi
K. A. Lele, A. A. Desai, S.A. Shaikh, S. Agrawal
PG Student, EXTC, DJSCOE
Vile Parle, Mumbai, India

ABSTRACT
The variation of circular microstrip antenna, a Sectoral microstrip antenna is discussed. The detail analysis to study the effects of antenna parameters like, feed point location and the substrate thickness for Sectoral angle increasing from 270^0 to 340^0 on the patch first four resonant modes is presented. The variation in angle tunes the spacing between three patch resonant modes which yields optimum simulated and measured bandwidth of more than 700 MHz (>60%) in 340^0 Sectoral patch. The Sectoral antenna variation yields broadside radiation pattern with antenna gain of more than 4 dBi over most of the bandwidth.

Keywords
Circular microstrip Antenna, Sectoral microstrip antenna, Broadband microstrip Antenna, Proximity feed, Higher order mode.

1. INTRODUCTION
Broadband microstrip antenna (MSA) is realized by fabricating the patch on lower dielectric thicker substrate in conjunction with the proximity feeding technique [1 – 4]. In most of the reported applications, patch is suspended in air above the finite ground plane thereby realizing unity value of dielectric constant. The thicker substrate greater than $0.06\lambda_0$ reduces the quality factor of the cavity below the patch whereas proximity feeding technique yields input impedance matching on thicker substrate which realizes broader bandwidth (BW). To further enhance the MSA BW, multi-resonator gap-coupled and stacked configurations have been used [4 – 7]. The multi-resonator configurations are simpler to design but they increase the overall antenna size. More commonly broadband MSAs are realized by cutting the slot of different shapes like, U-slot, rectangular slot and their modified variations at an appropriate position inside the patch [8 – 14]. The slot is said to introduce an additional resonant mode near the fundamental patch mode to realize broader bandwidth (BW). The slot cut MSA does not increase the patch size, but as compared to multi-resonator configurations, they are complex in design. Without using additional parasitic patch or slot, the antenna BW is increased by varying one of the patch parameter like, Sectoral angle in Sectoral MSA (S-MSA) [15]. The Sectoral angle tunes the spacing between patch resonant modes to realize broader BW [15]. By tuning first two patch resonant modes with the help of rectangular slot, BW of 270^0 S-MSA has been increased [16]. In this paper, an analysis to study the effect of variation in Sectoral angle of S-MSA on its first four resonant modes is presented. Initially fundamental and higher order modes of circular MSA and its equivalent S-MSAs for Sectoral angle increasing from 270^0 to 340^0 are discussed. The parametric study for variation in Sectoral angle, substrate thickness of coupling strip and its position below the patch is presented. The increase in Sectoral angle tunes the first three S-MSA resonant mode frequencies and thereby reduces the spacing between them. The results for first three resonant mode frequencies and their ratio are tabulated. The variation in coupling strip thickness alters the capacitive impedance formed between the patch and strip which changes the position of loop in the input impedance locus. The input impedance variation across various modes in S-MSA over the Sectoral area is different. The variation in strip position changes the coupling between patch modes and the strip which affects the loop size in the input impedance locus. Using the above parametric study the optimum spacing between three resonant modes is obtained in 340^0 S-MSA which gives broader BW of more than 700 MHz (>60%) [17]. However over the three resonant modes, orthogonal variations in surface current components was observed that gives higher cross polar levels towards lower and higher frequencies of the BW [17]. Hence the antenna gain in 340^0 S-MSA is more than 4 dBi over most of the BW. The analysis of S-MSAs for varying angle was carried out using IE3D software on finite square ground plane of side length 30 cm [18]. The measurements for optimum 340^0 S-MSA as given in [17] has been carried out to validate the simulated result. The antenna is fabricated using copper plate having finite thickness and is supported in air using foam spacer support placed towards the antenna corners. The antenna is fed using N-type connector of 0.32 cm inner wire diameter and input impedance response was measured using R & S Vector network analyzer (ZVH – 8). The antenna radiation pattern and gain were measured using RF source (SMB – 100A) and spectrum analyzer (FSC – 6). The measurement was carried out by ensuring required minimum far field distance between reference antenna and antenna under test, with reference to the lower frequency of the BW. The antenna gain is measured in the co-polar direction using two antenna method.

2. ANALYSIS OF PROXIMITY FED S-MSAs
The proximity fed circular MSA and equivalent S-MSA on air substrate of thickness h = 3.0 cm and strip thickness of h_1 = 2.8 cm are shown in Fig. 1(a – c). The patch radius in CMSA is calculated such that it resonates in its TM_{11} mode at frequency of around 950 MHz [1 – 4]. This frequency band is chosen as % antenna BW is small in this range. The thicker air substrate is selected as it realizes maximum radiation efficiency. The proximity feeding technique is used since it is the simplest method to implement while using thicker air substrate. The proximity fed CMSA is simulated over 700 to 2500 MHz frequency band for x_f = 3.5 and y_f = 0, and its resonance curve plot is shown in Fig. 1(d). The plots shows peaks due to fundamental TM_{11} and higher order TM_{21}, TM_{02} modes. The surface currents at TM_{11} mode shows one half

wavelength variations along patch diameter and half of the patch perimeter [1 – 4]. At TM_{21} mode, currents show two half wavelength variation along half of the patch perimeter and one half wavelength variation along patch diameter [1 – 4]. The surface current shows two half wavelength variations along patch diameter and no variation along the patch perimeter at TM_{02} mode [1 – 4]. The S-MSA of the same patch radius is simulated for different Sectoral angle and resonance curve plots and input impedance plots for them are shown in Fig. 2(a – c) and 3(a), respectively. The frequencies of first three resonant modes and their ratio for angle increasing from 270^0 to 340^0 are given in Table 1 and 2, respectively. The surface current distribution at first three resonant modes in 270^0 and 300^0 S-MSA are shown in Fig. 3(b – d) and 4(a – c), respectively. In all the S-MSAs an additional resonant mode (TM_{10}) is present below the fundamental TM_{11} mode of equivalent CMSA. At this mode the surface current shows one half wavelength variations along patch perimeter. At second mode, surface current shows half wave length variation along half of the patch perimeter. This mode is similar to TM_{11} mode in CMSA. The next mode is equivalent to TM_{21} mode as surface current shows two half wavelength variation along half of the patch perimeter. The equivalent TM_{11} and TM_{21} mode frequencies in S-MSA are higher than that of TM_{11} and TM_{21} mode frequencies in CMSA. However for higher angles, TM_{11} and TM_{21} mode frequencies in S-MSA approaches the frequencies in CMSA.

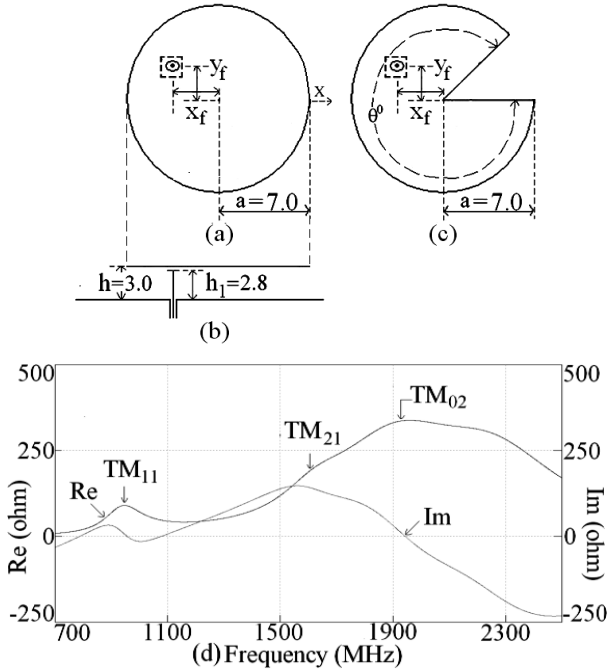

Fig 1: (a) Top and (b) side views of proximity fed CMSA, (c) proximity fed S-MSA of angle 'θ' and (d) resonance curve plot for CMSA

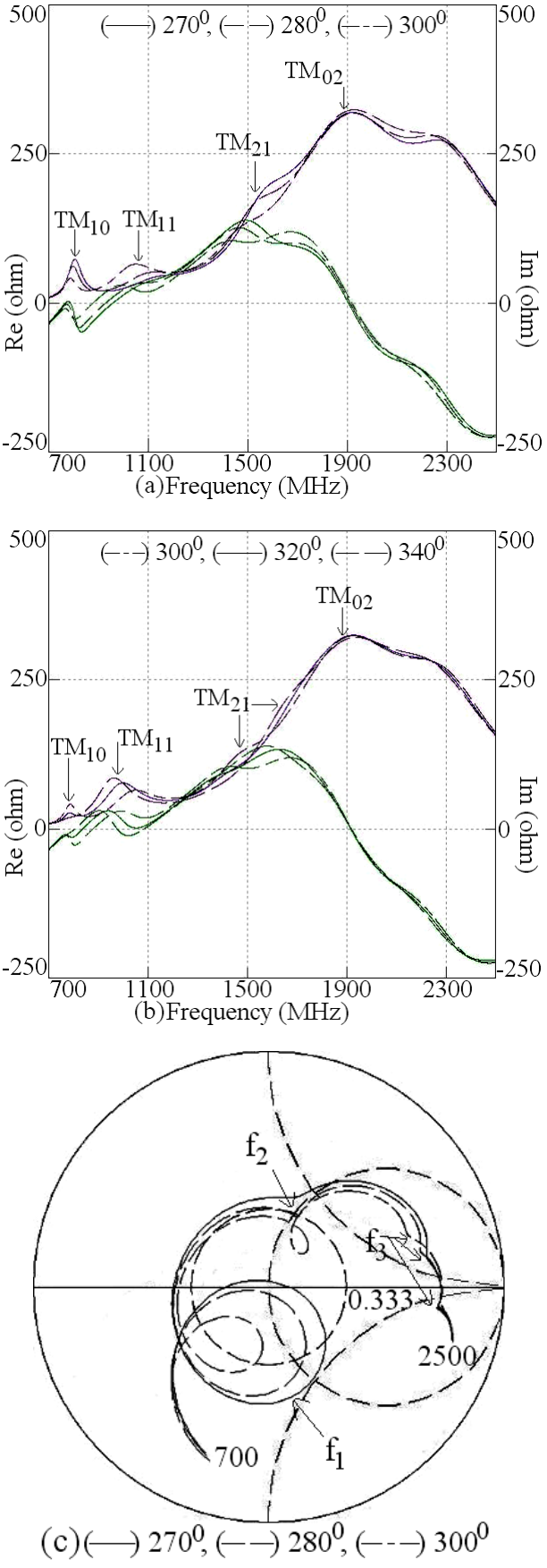

Fig 2 (a, b) Resonance curve and (c) input impedance plots for varying Sectoral angle for S-MSA

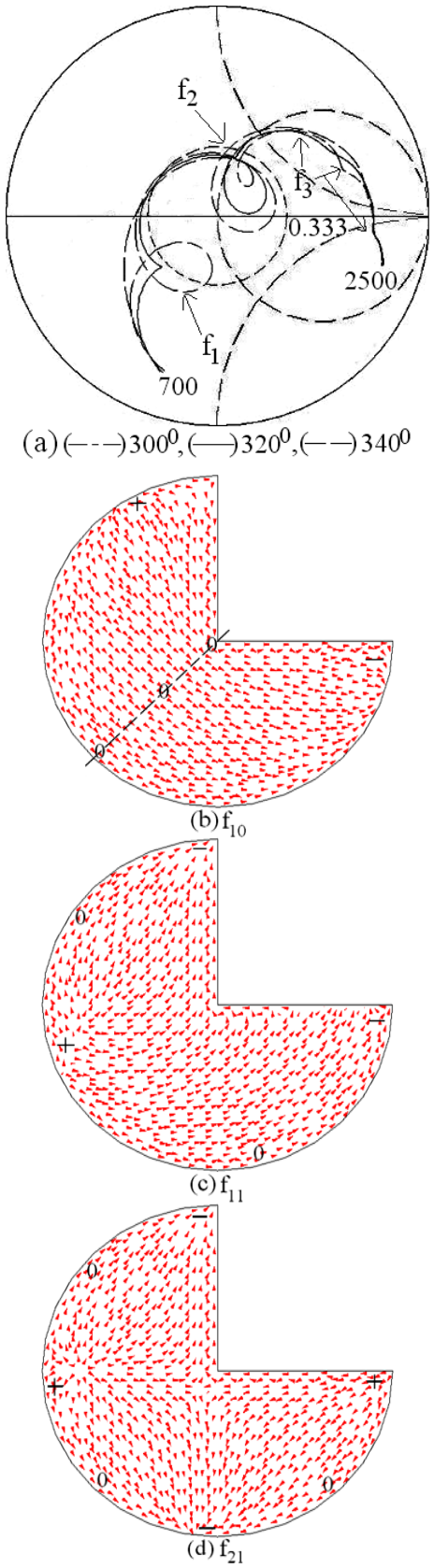

Fig 3 (a) Input impedance plots for varying Sectoral angle for S-MSA and (b – d) surface current distribution at three resonant modes for 270^0 S-MSA

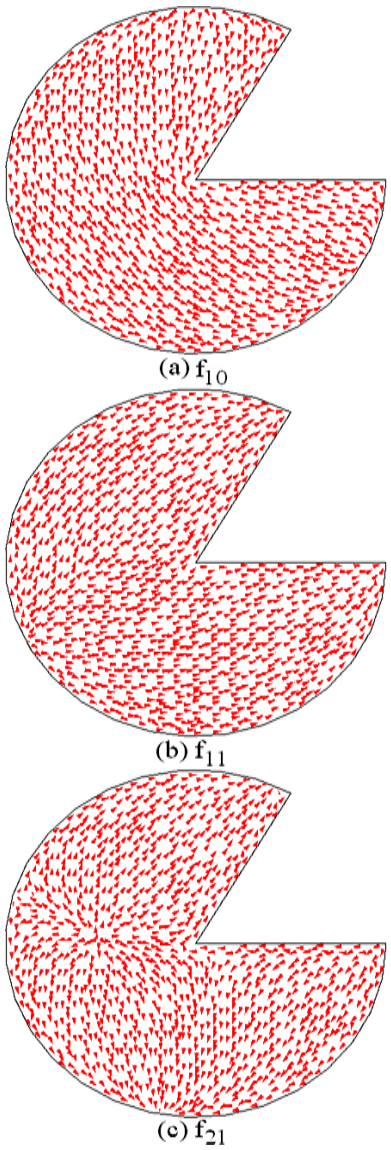

Fig 4 (a – c) Surface current distribution at three resonant modes for 300^0 S-MSA

Table 1 – Variation of first three mode resonance frequencies against Sectoral angle in S-MSA

θ^0	f_1 (MHz)	f_2 (MHz)	f_3 (MHz)
270^0	805	1141	1580
280^0	798	1112	1544
300^0	787	1054	1473
320^0	784	998	1428
340^0	779	964	1369

Table 2 – Variation of frequency ratio against variation in Sectoral angle for S-MSA

θ^0	f_2/f_1	f_3/f_1	f_3/f_2
270^0	1.42	1.96	1.38
280^0	1.39	1.93	1.39
300^0	1.34	1.87	1.39
320^0	1.27	1.82	1.43
340^0	1.24	1.76	1.42

With increase in Sectoral angle, contribution of surface currents over three modes increases along the horizontal direction inside the Sectoral patch. The input impedance and resonance curve plots for variation in substrate thickness for coupling strip is shown in Fig. 5(a, b).

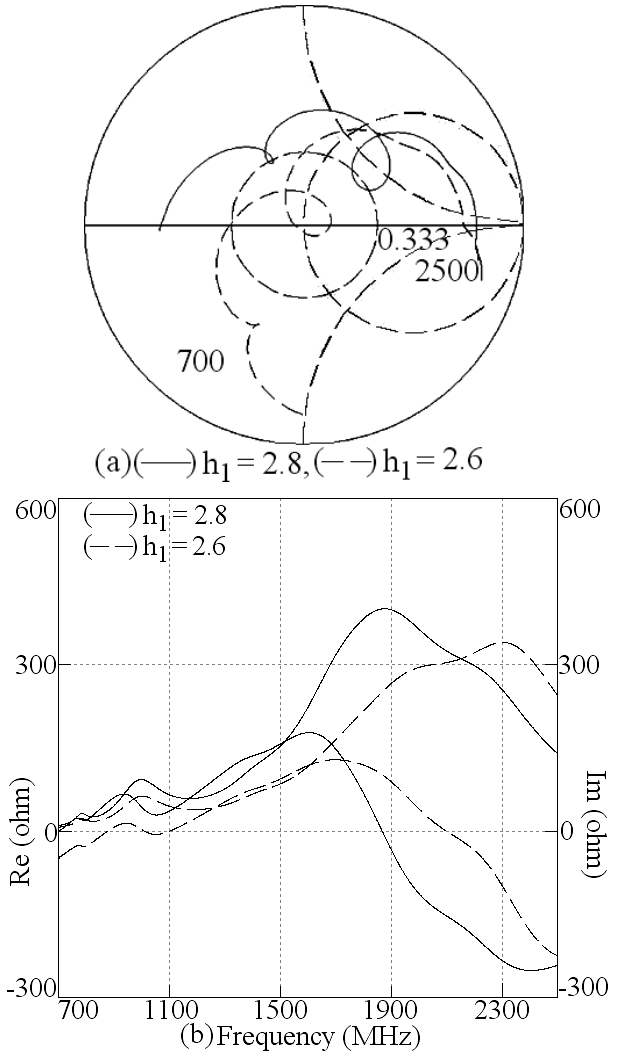

Fig 5 (a) Input impedance and (b) resonance curve plots for 300^0 S-MSA for variation in coupling strip thickness

The decrease in 'h_1', increases capacitive impedance formed between patch and strip that rotates the input impedance locus in anti-clockwise direction inside the smith chart. The reduction in 'h_1' also reduces the impedance at all the modes. This yields broadband response with formation of loop inside VSWR = 2 circle at TM_{11} mode in S-MSA. The input impedance and resonance curve plots for varying feed point location is shown Fig. 6(a, b).

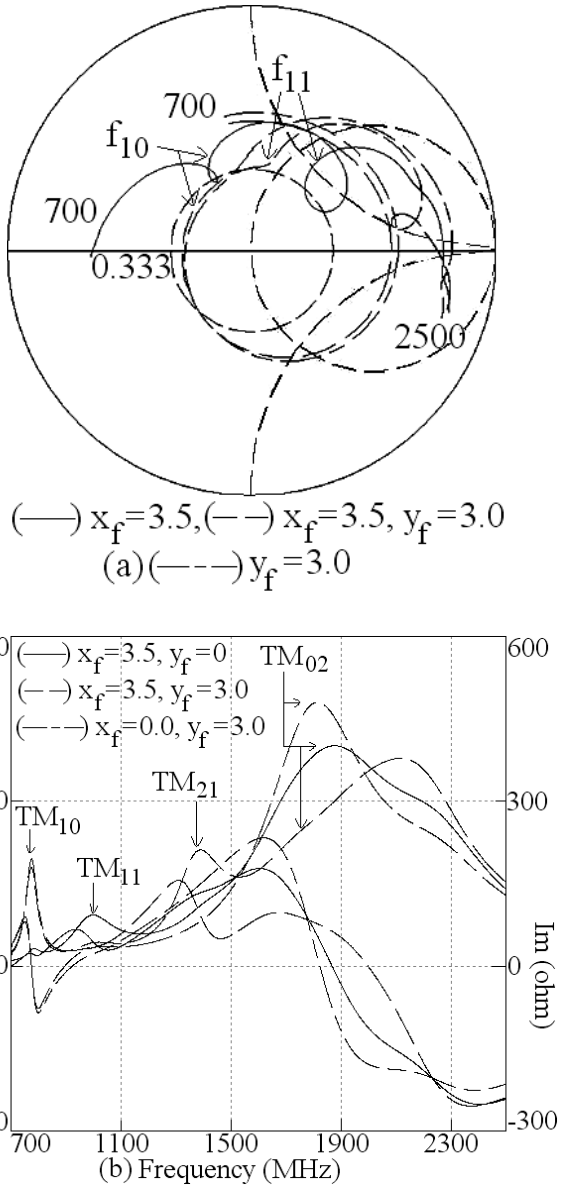

Fig 6 (a) Input impedance and (b) resonance curve plots for 300^0 S-MSA for variation in proximity feed location

At TM_{10} mode in 300^0 S-MSA, the loop size increases when the feed point is shifted away from horizontal axis. This is because the impedance increases at TM_{10} mode for moving away from x-axis. The loop at TM_{11} and TM_{21} mode reduces since the feed is placed near the minimum impedance location at those modes. Thus the loop size at individual mode can be controlled by suitably selecting the feed point location which will help in to control the BW at individual modes. With increase in Sectoral angle from 270^0 to 340^0, ratio between first three resonant modes reduces. By suitably selecting the proximity feed point location below the patch, broadband response has been realized in 340^0 S-MSA [17]. It gives simulated and measured BW of 736 MHz (66%) and 745

MHz (66.1%), respectively as shown in Fig. 7(a) [17]. Due to orthogonal variations in surface currents over three resonant modes, measured gain in 340^0 S-MSA varies from more than 7 dBi to around 4 dBi over the BW [17]. The fabricated prototype of the configuration is shown in Fig. 7(b).

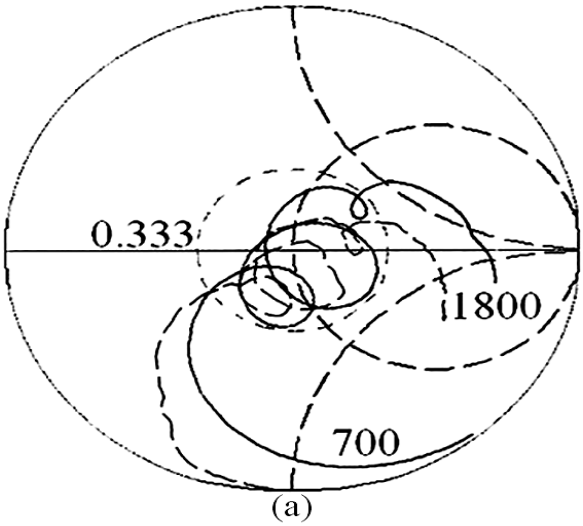

(a)

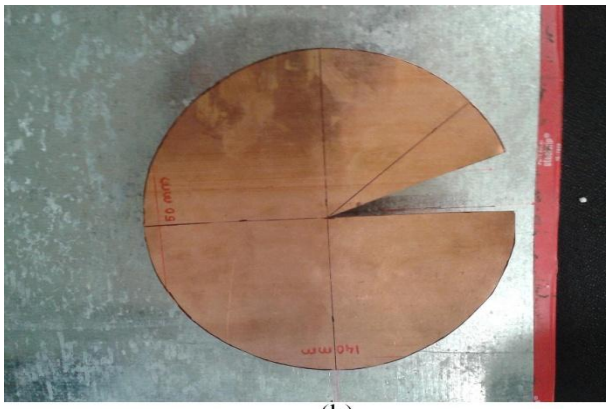

(b)

Fig. 4 (a) Input impedance plots, (—) simulated, (— —) measured [17] and (b) fabricated prototype of for proximity fed 340^0 S-MSA [17]

3. CONCLUSIONS

The detail analysis of S-MSA derived from CMSA for variation in Sectoral angle, substrate thickness for strip, feed point location and by studying the surface current distribution is presented. The increase in Sectoral angle reduces the spacing and frequency ratio between first three patch resonant modes. The variation in strip thickness optimizes the impedance at various modes as well as optimizes the loop position inside VSWR = 2 circle. The feed point location helps to control the loop size. The increase in Sectoral angle increases the contribution of surface currents along one dimension over the Sectoral patch. The broader BW of more than 700 MHz (>65%) is obtained in 340^0 S-MSA.

4. REFERENCES

[1] Garg, R., Bhartia, P., Bahl, I., and Ittipiboon, A., *Microstrip Antenna Design Handbook*, Artech House, USA, 2001.

[2] Bhartia, B., and Bahl, I. J., *Microstrip Antennas*, USA, 1980.

[3] Cock, R. T., and Christodoulou, C. G., Design of a two layer capacitively coupled, microstrip patch antenna element for broadband applications, IEEE Antennas Propag. Soc. Int. Symp. Dig., vol. 2, 1987, pp. 936-939.

[4] Kumar, G., and Ray, K. P., *Broadband Microstrip Antennas*, Artech House, 2003.

[5] Deshmukh, Amit A., and Kumar, G., Compact Broadband gap-coupled Shorted L-shaped Microstrip Antennas, Microwave and Optical Technology Letters, vol. 47, no. 6, 20th Dec. 2005, pp. 599 – 605.

[6] Deshmukh, Amit A., and Kumar, G., Compact Broadband stacked Microstrip Antennas, Microwave and Optical Technology Letters, vol. 48, no. 1, Jan. 2006, pp. 93 – 96.

[7] Ray, K. P., Sevani, V. and Deshmukh, Amit A., Compact gap-coupled microstrip antennas for broadband and dual frequency operations, International Journal of Microwave and Optical Technology, vol. 2, no. 2, July 2007, pp. 193 – 202.

[8] Wong, K. L., *Compact and Broadband Microstrip Antennas*, John Wiley & sons, Inc., New York, USA, 2002.

[9] Huynh, T., and Lee, K. F., Single-Layer Single-Patch Wideband Microstrip Antenna, Electronics Letters, vol. 31, no. 16, August 1995, pp. 1310-1312.

[10] K. L. Wong and W. H. Hsu, "A broadband rectangular patch antenna with a pair of wide slits", IEEE Trans. Antennas Propagat., vol. 49, Sept. 2001, pp. 1345 – 1347

[11] Lee, K. F., Yang, S. L. S., Kishk, A. A., and Luk, K. M., The Versatile U-slot Patch, IEEE Antennas & Propagation Magazine, vol. 52, no. 1, February 2010, pp. 71 – 88.

[12] Guo, Y. X., Luk, K. M., Lee, K. F. and Chow, Y. L., Double U-slot Rectangular Patch Antenna, Electronics Letters, vol. 34, 1998, pp. 1805 – 1806.

[13] Sharma, S. K., and Shafai, L., Performance of a Novel Ψ-Shaped Microstrip Patch Antenna with Wide Bandwidth, IEEE Antennas & Wireless Propagation Letters, vol. 8, 2009, pp. 468 –471.

[14] Clenet, M., and Shafai, L., Multiple resonances and polarization of U-slot patch antenna, Electronics Letters, vol. 35, no. 2, 21st January 1999, pp.101 – 102.

[15] Deshmukh, A. A., Jain, A. R., Joshi, A. A., Tirodkar, T. A. and Ray, K. P., Broadband Proximity fed modified Circular Microstrip Antenna", Proceedings of ICACC – 2013. (DOI - 10.1109/ICACC.2013.87)

[16] Deshmukh, Amit A., Jain, Ankita R., and Ray, K. P., Broadband 270^0 Sectoral Microstrip Antenna, Microwave and Optical Technology Letters, vol. 56, no. 6, June 2014, pp. 1447 – 1449, (DOI: 10.1002/mop.28351).

[17] Deshmukh, Amit A., and Phatak, Neelam V., Broadband Sectoral Microstrip Antennas, IEEE Antennas and Wireless Propagation Letters, vol. 14, pp. 727 – 730, 2015. (DOI - 10.1109/LAWP.2014.2385108)

[18] IE3D 12.1, Zeland Software, Fremont, USA, 2004.